



LAWRENCE
LIVERMORE
NATIONAL
LABORATORY

Improved calibration of the OMEGA gas Cherenkov detector

A. B. Zylstra, H. W. Herrmann, Y. H. Kim, A. McEvoy,
K. Meaney, V. YU. Glebov, C. Forrest, M. Rubery

September 16, 2019

Review of Scientific Instruments

Disclaimer

This document was prepared as an account of work sponsored by an agency of the United States government. Neither the United States government nor Lawrence Livermore National Security, LLC, nor any of their employees makes any warranty, expressed or implied, or assumes any legal liability or responsibility for the accuracy, completeness, or usefulness of any information, apparatus, product, or process disclosed, or represents that its use would not infringe privately owned rights. Reference herein to any specific commercial product, process, or service by trade name, trademark, manufacturer, or otherwise does not necessarily constitute or imply its endorsement, recommendation, or favoring by the United States government or Lawrence Livermore National Security, LLC. The views and opinions of authors expressed herein do not necessarily state or reflect those of the United States government or Lawrence Livermore National Security, LLC, and shall not be used for advertising or product endorsement purposes.

Improved calibration of the OMEGA gas Cherenkov detector

A.B. Zylstra,^{1, a)} H.W. Herrmann,² Y.H. Kim,² A. McEvoy,² K. Meaney,² V.Yu. Glebov,³ C. Forrest,³ and M. Rubery⁴

¹⁾Lawrence Livermore National Laboratory, Livermore, CA 94550 USA

²⁾Los Alamos National Laboratory, Los Alamos, NM 87545 USA

³⁾Laboratory for Laser Energetics, University of Rochester, Rochester, NY 14623 USA

⁴⁾Plasma Physics Department, AWE plc, Reading RG7 4PR, United Kingdom

Inertial fusion implosions are diagnosed using γ rays to characterize the implosion physics or measure basic nuclear properties, including cross sections. For the latter, previously reported measurements at laser facilities using gas Cherenkov detectors are limited by a large systematic uncertainty in the detector response. We present a novel in-situ calibration technique using neutron inelastic scattering, which we apply to the new GCD-3 detector. The calibration accuracy is improved by $\sim 3\times$ over the previous method.

I. INTRODUCTION

Detecting γ rays produced by nuclear reactions occurring during laser-driven inertial confinement fusion (ICF)¹ experiments is important for diagnosing aspects of the implosion physics^{2–5}, and for studying nuclear reactions^{6–8}. γ -ray detectors at ICF facilities are primarily based on the Cherenkov mechanism⁹, including the gas Cherenkov detectors (GCD)^{10,11} and Gamma Reaction History (GRH)¹². The GCDs, described extensively in Refs. 10,11, are placed inside the target chamber; the front face contains a low- Z converter in which incident γ rays Compton scatter electrons into a gas cell where they produce Cherenkov light, which is collected by a Cassegrain optics system onto a photomultiplier tube (PMT).

In studies of nuclear physics cross sections, an absolute calibration of the instrument is required. Previous work using the first iteration of GCD (GCD-1) to measure γ -producing reactions, for example Refs. 6–8 used an *in-situ* calibration method against the D³He reaction using separate diagnostics to measure the proton yield combined with the γ/p branching ratio¹³. The latter has a large uncertainty, $\sim 35\%$, which then propagates into inferred quantities including the DT fusion γ/n branching ratio^{6,7} and the T³He cross section for production of ⁶Li, an astrophysically-important reaction⁸.

The γ -ray yield of a reaction x (Y_x) can be calculated from the integrated signal ($V \times s$) measured by one of the Cherenkov detectors using the detector equation

$$Y_x = \frac{V \times s}{\Omega \times R \times e \times QE \times G} \times \frac{\chi}{C_x}, \quad (1)$$

where Ω is the detector solid angle, R is the scope input impedance (50 Ohm), e is the fundamental charge, QE is the PMT quantum efficiency, and G is the PMT gain.

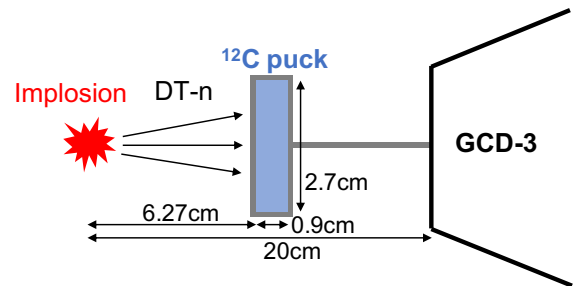


FIG. 1: Calibration geometry. An implosion (left) generates DT neutrons, which are incident on a puck of ¹²C placed between the implosion and the GCD.

C_x is the effective GCD response for reaction x in photons collected per incident γ , which is calculated using Geant4 Monte-Carlo simulations¹⁴. χ is the overall detector efficiency calibration factor, which we infer in this work, and mainly results from deficiencies in the Geant4 model to accurately capture collection and transport of the Cherenkov light in the physical instrument.

In this paper, we report a new calibration inferred from *in-situ* measurements of neutron inelastic scattering on a ¹²C puck placed near the detector. This method is conceptually similar to the method used to infer an effective response for the γ -ray detectors to carbon areal density¹⁵, except in this case we use available nuclear data from accelerator experiments to infer the calibration factor. We report a calibration factor for the new GCD-3^{11,16} which is accurate to $\pm 12\%$, a substantial improvement, by about a factor of $3\times$, over the previous D³He technique.

II. ¹²C PUCK DATA

In the calibration scheme, a puck of ¹²C graphite of known areal density is placed in front of the instrument and exposed to 14.1 MeV neutrons generated by an implosion filled with DT fuel. The DT-n inelastically scat-

^{a)}Electronic mail: zylstra1@llnl.gov

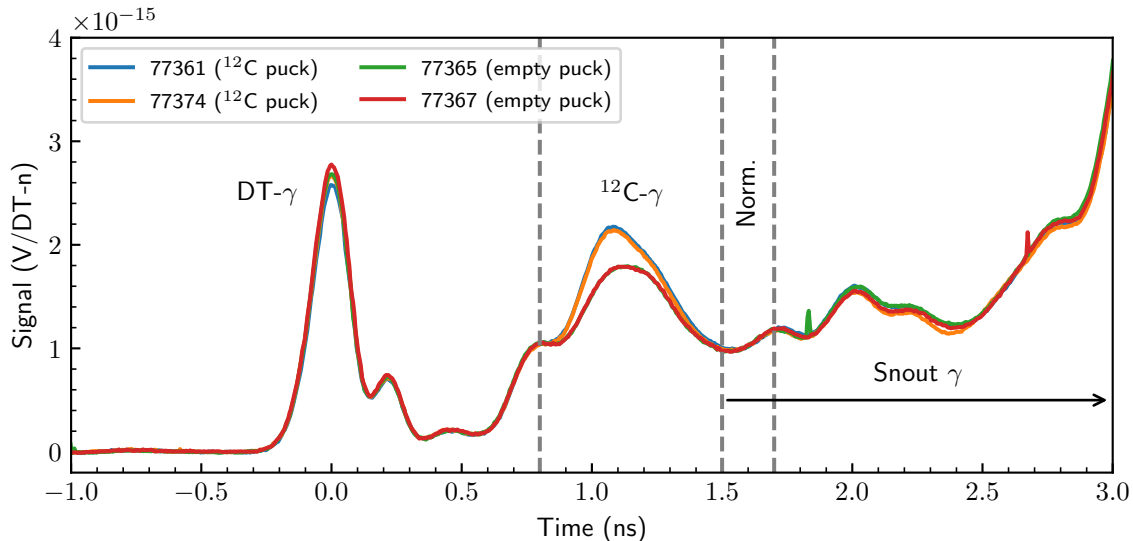


FIG. 2: Calibration data, consisting of two shots with a ^{12}C puck (77361 and 77374) and two background shots (77365 and 77367) with an empty puck holder. The signal at $t = 0$ is from direct DT fusion γ s, the puck signal comes between $0.8 \rightarrow 1.5$ ns, and signal from (n, γ) reactions on other diagnostic snout hardware occurs later in time. The signals are normalized to the snout signal between $1.5 \rightarrow 1.7$ ns.

ter in the carbon ‘puck’, generating a signal in the γ detector from the 4.4 MeV γ -ray line. The experimental geometry is shown in Fig. 1. A puck holder, 2.7cm in diameter and 0.9cm deep, is filled with ^{12}C powder with a total mass of 5.52g. The front of the carbon puck is 6.27cm from the implosion. The carbon is held in a beryllium case with a thickness of 1.2mm on the front and rear.

Data from calibration shots on the OMEGA laser facility¹⁷ are shown in Fig. 2, including two background shots where the puck assembly does not contain ^{12}C , and two calibration shots with the ^{12}C sample. The data are time-aligned so that the DT- γ peak is at $t = 0$. Based on the neutron time of flight to the sample, the puck signal occurs at ~ 1.1 ns. Since some (n, γ) reactions occur in the hardware that holds the puck, the ‘empty’ puck shots show some background signal that must be subtracted from the ^{12}C shots to obtain the signal due only to ^{12}C inelastic scattering. Later in time, from approximately 1.5 ns onwards, there is additional Cherenkov signal generated by neutron inelastic scattering in other materials in the target chamber, predominantly diagnostic ‘snouts’ close to the implosion. The configuration of this hardware is kept constant so that it can be subtracted.

The empty puck background is subtracted from the two ^{12}C shots; the background-subtracted signals shown in Fig. 3. These traces represent the signal from carbon inelastic scattering, with a total signal obtained by integrating the data from 0.8 to 1.5 ns (gray dashed lines).

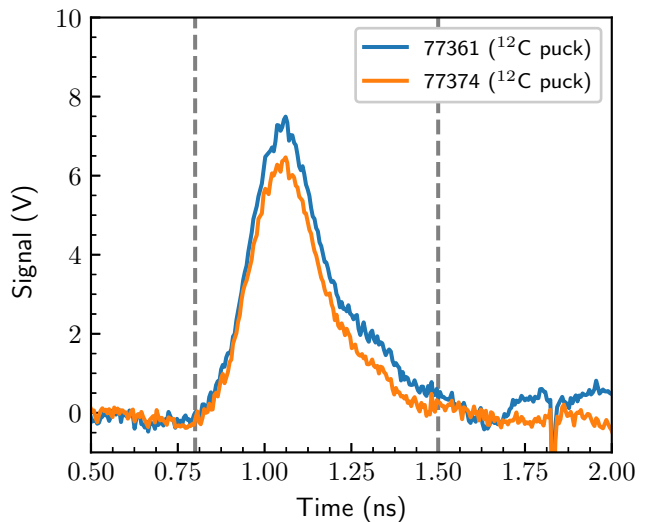


FIG. 3: GCD data from the two carbon puck shots after background subtraction. The integration period is from 0.8 to 1.5 ns.

III. INFERRED CALIBRATION FACTOR

The calibration factor can be inferred from the integrated signal ($V \times s$) using Eq. 1 with the number of carbon γ s incident on the detector. This can be calculated using the DT neutron yield, which is measured using nuclear activation and scintillator-based detectors^{18,19}, and the differential cross section for neutron inelastic scatter-

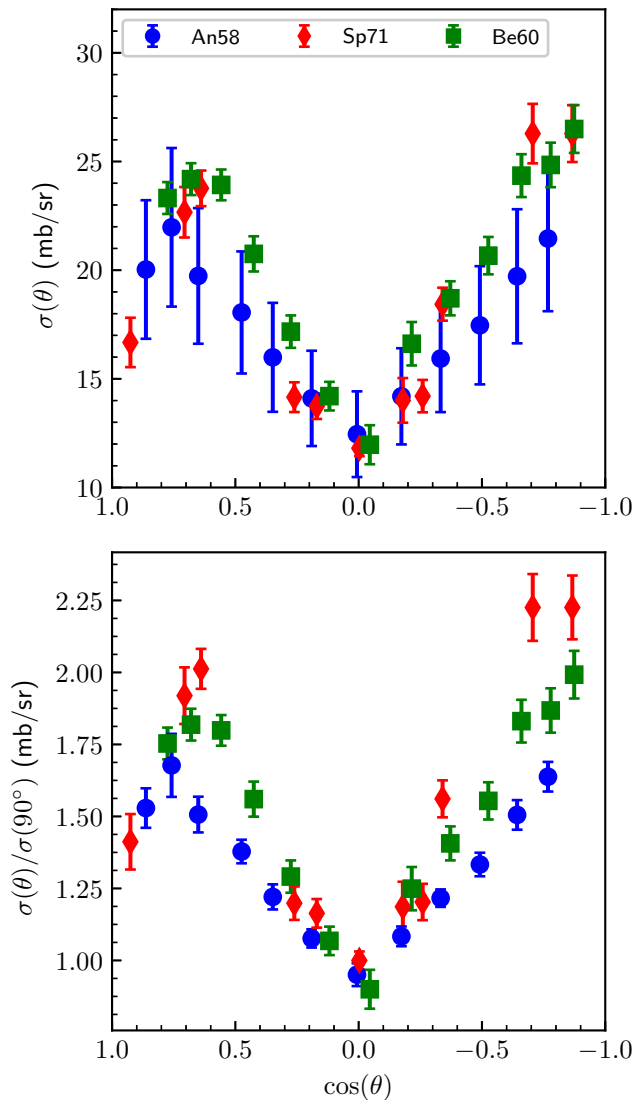


FIG. 4: Published data on ^{12}C inelastic scattering from Refs. 20–22.

ing on ^{12}C .

Published data^{20–22} on neutron inelastic scattering on ^{12}C is shown in Fig. 4 as absolute (top) and relative (bottom) values of the differential cross section. A strong angular anisotropy is observed in the differential cross section, which will affect the inferred calibration factor using this technique.

Typically the angular distribution is described by a fit of the form

$$\sigma(\theta) = \sigma(90^\circ) [1 + a \cos^2(\theta) - b \cos^4(\theta)]. \quad (2)$$

While best-fit values with uncertainties are reported in Refs. 20–22 for $\sigma(90^\circ)$, a , and b , the full correlation matrices are not reported, yet are important - especially for a and b . We therefore re-fit the raw data from Refs. 20–22 using Eq. 2. The best-fit differential cross sections

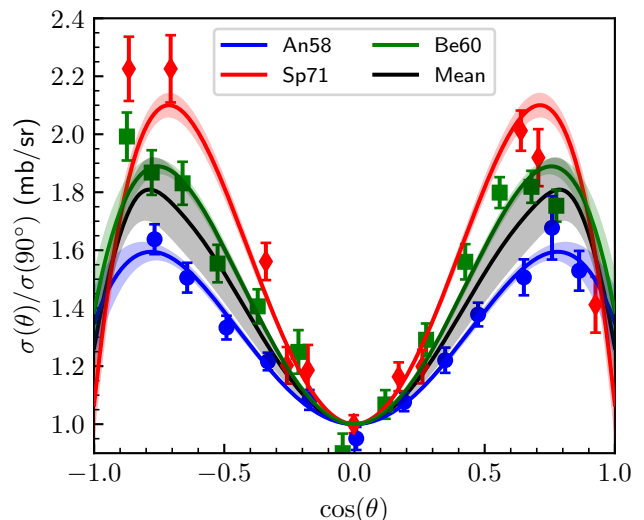


FIG. 5: Fits to the differential cross section data as well as adopted mean.

are shown in Fig. 5

The three data sets show a clear discrepancy, especially near the peaks at $\sim 45^\circ$. To create a single adopted differential cross section, we use a weighted mean of the three values at each value of $\cos(\theta)$,

$$\sigma(\theta) = \frac{\sum_i \sigma_i(\theta) \delta\sigma_i(\theta)^{-2}}{\sum_i \delta\sigma_i(\theta)^{-2}} \quad (3)$$

where i denotes our fit to each of the three data sets (Refs. 20–22), and $\delta\sigma_i$ is the uncertainty from our fits. The uncertainty in the mean is taken as

$$\delta\sigma(\theta) = \sqrt{\frac{1}{\sum_i \delta\sigma_i(\theta)^{-2}} + \frac{1}{N^2} \sum_i (\sigma(\theta) - \sigma_i(\theta))^2} \quad (4)$$

The first term in the square root represents the weighted mean's uncertainty. We add in quadrature the typical standard deviation of the mean (with $N = 3$) in the second term to account for the fact that the variance within each data set is a clear underestimate of the deviation in shape between data sets. The resulting mean value ($\sigma(\theta)$) is plotted in Fig. 5, with the uncertainty ($\delta\sigma(\theta)$) shown by the shaded region. We also calculate the total cross section as 217.5 ± 5.5 mb.

With this differential cross section we calculate a geometric efficiency factor f_1 , following Ref. 15, which accounts for the scattering angles that result in the γ ray incident on the face of the GCD-3. This factor is obtained by integrating the normalized differential cross section over the face of the detector, which gives $f_1 = 1.369 \pm 0.089$. This can then be combined with a rewritten version of Hoffman's Eq. 1 and our Eq. 1 to

obtain an expression for the GCD-3 calibration factor,

$$\frac{1}{\chi} = \frac{1}{Y_n} \frac{V \times s}{\Omega \times R \times e \times \text{QE} \times G} \frac{1}{R_{p,\gamma}} \frac{m_C}{\sigma} \frac{4\pi D^2}{M_{puck}} \frac{1}{f_1} \quad (5)$$

where σ is the total cross section, f_1 accounts for the angular anisotropy, m_C is the mass of a carbon nucleus, D is the puck distance, and M_{puck} is the total puck mass. $R_{p,\gamma}$ is the number of Cherenkov photons detected by the PMT per incident γ ray, and is calculated using GEANT4 for the 4.44 MeV γ ray characteristic of inelastic scattering on ^{12}C . The expression in Eq. 5 uses the measured neutron yield on a shot with the known geometry and nuclear physics quantities to infer the number of γ s incident on the detector from inelastic scattering, which when combined with the known detector quantities determines, empirically, the calibration factor. For each shot the random uncertainty largely results from Y_n , since the signal integration has a negligible contribution. Systematic uncertainties result from σ , f_1 , M_{puck} , D , and the PMT response ($\text{QE} \times G$).

Finally, a correction for the attenuation of both the incident neutrons and outgoing γ rays in the puck and puck holder is included. The incident DT neutrons are attenuated by $\sim 5.4\%$ in the beryllium puck holder and half of the puck material, while the outgoing γ s are attenuated by $\sim 2\%$ in half of the puck material and the puck holder. Including the self-attenuation correction, we take a weighted mean of the two shots, finding $\chi = 0.56 \pm 0.07$.

IV. GCD-3 D³HE CALIBRATION

Data on the GCD-3 to use the old D³He cross-calibration technique are also available. Three D³He-filled implosions are used in this calibration. The raw data are shown in Fig. 6. These data are analyzed by calculating the total signal and inverting Eq. 1 to obtain χ . The total γ -ray yield from D³He is calculated using a published value of the γ/p branching ratio¹³ and measurements of the proton yield from WRF spectrometers²³.

In this calibration, the signal uncertainty is dominated by statistical uncertainty from the number of productive Compton-scattered electrons in the system, which is the statistically-limiting step of the Cherenkov detector technique. The statistical uncertainty in the D³He proton yield measurement is also included. The major source of uncertainty is from the uncertainty in the D³He branching ratio¹³. The calibration factor is calculated as a weighted mean of the three D³He shots and found to be 0.50 ± 0.20 , which is consistent with our value using the new ^{12}C calibration technique, albeit with a substantially larger uncertainty. A comparison of the inferred calibration factors from the two techniques is plotted in Fig. 7.

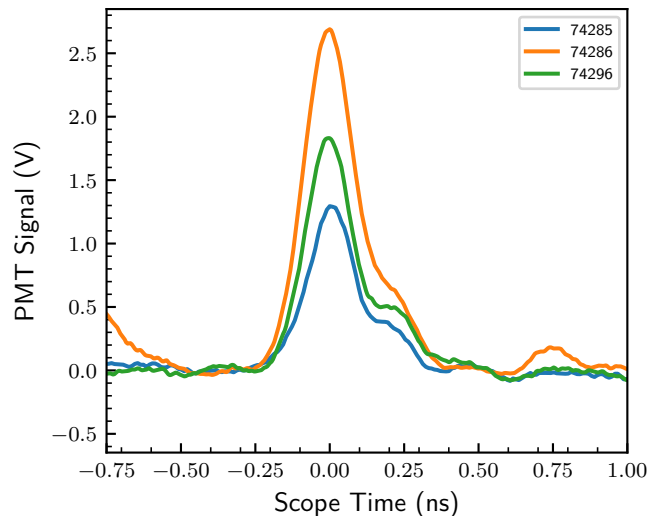


FIG. 6: GCD data from D³He fuel implosions.

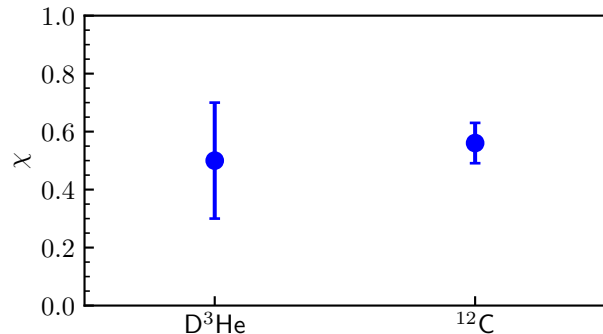


FIG. 7: Comparison of the inferred χ from the old calibration technique (D³He) compared to this method (^{12}C).

V. CONCLUSION

Absolute calibration of Cherenkov detectors used at laser-fusion facilities, including OMEGA and the NIF, is important, especially for measurements of absolute cross sections for nuclear reactions (e.g. Refs 6–8). These studies used the D³He reaction as a cross-calibration, which is severely limited in precision. Here we present a new technique, utilizing *in-situ* cross-calibration to inelastic scattering on a ^{12}C puck, which we apply to the newest GCD-3 on OMEGA. When combined with nuclear data, an absolute calibration factor can be inferred with an improvement of about $\sim 3\times$ compared to the D³He method. This technique is more broadly applicable to other Cherenkov-based detectors, and the uncertainty could be further reduced through improved nuclear data on ^{12}C neutron inelastic scattering.

ACKNOWLEDGMENTS

We thank the operations crews and engineering staff at OMEGA for supporting these experiments. This work was performed under the auspices of the U.S. Department of Energy by Lawrence Livermore National Laboratory in part under Contract DE-AC52-07NA27344, by Los Alamos National Laboratory under Contract No. DE-AC52-06NA52396, and supported by the U.S. DOE Early Career Research Program (Fusion Energy Sciences) under FWP SCW1658.

This document was prepared as an account of work sponsored by an agency of the United States government. Neither the United States government nor Lawrence Livermore National Security, LLC, nor any of their employees makes any warranty, expressed or implied, or assumes any legal liability or responsibility for the accuracy, completeness, or usefulness of any information, apparatus, product, or process disclosed, or represents that its use would not infringe privately owned rights. Reference herein to any specific commercial product, process, or service by trade name, trademark, manufacturer, or otherwise does not necessarily constitute or imply its endorsement, recommendation, or favoring by the United States government or Lawrence Livermore National Security, LLC. The views and opinions of authors expressed herein do not necessarily state or reflect those of the United States government or Lawrence Livermore National Security, LLC, and shall not be used for advertising or product endorsement purposes.

- ¹J. Nuckolls, L. Wood, A. Thiessen, and G. Zimmerman, *Nature* **239**, 139 (1972).
- ²H. W. Herrmann, J. M. Mack, C. S. Young, R. M. Malone, W. Stoeffl, and C. J. Horsfield, *Rev. Sci. Instrum.* **79**, 10E531 (2008).
- ³H. W. Herrmann, N. Hoffman, D. Wilson, W. Stoeffl, L. Dauffy, Y. Kim, A. McEvoy, C. Young, J. Mack, C. Horsfield, *et al.*, *Rev. Sci. Instrum.* **81**, 10D333 (2010).
- ⁴A. B. Zylstra, H. W. Herrmann, Y. H. Kim, A. McEvoy, M. J. Schmitt, G. Hale, C. Forrest, V. Y. Glebov, and C. Stoeckl, *Rev. Sci. Instrum.* **88**, 053504 (2017).
- ⁵A. Zylstra, H. Herrmann, Y. Kim, K. Meaney, H. Geppert-Kleinrath, M. Schmitt, N. Hoffman, A. Leatherland, and S. Gales, *Rev. Sci. Instrum.* **89**, 10I103 (2018).
- ⁶Y. Kim, J. Mack, H. Herrmann, C. Young, G. Hale, S. Caldwell, N. Hoffman, S. Evans, T. Sedillo, A. McEvoy, J. Langenbrunner, H. Hsu, M. Huff, S. Batha, C. Horsfield, M. Rubery, W. Garbett, W. Stoeffl, E. Grafil, L. Bernstein, J. Church, D. Sayre, M. Rosenberg, C. Waugh, H. Rinderknecht, M. G. Johnson, A. Zylstra, J. Frenje, D. Casey, R. Petrasso, E. K. Miller, V. Y. Glebov, C. Stoeckl, and T. Sangster, *Phys. Plasmas* **19**, 056313 (2012).
- ⁷Y. Kim, J. M. Mack, H. W. Herrmann, C. S. Young, G. M. Hale, S. Caldwell, N. M. Hoffman, S. C. Evans, T. J. Sedillo, A. McEvoy, J. Langenbrunner, H. H. Hsu, M. A. Huff, S. Batha, C. J. Horsfield, M. S. Rubery, W. J. Garbett, W. Stoeffl, E. Grafil, L. Bernstein, J. A. Church, D. B. Sayre, M. J. Rosenberg, C. Waugh, H. G. Rinderknecht, M. Gatu Johnson, A. B. Zylstra, J. A. Frenje, D. T. Casey, R. D. Petrasso, E. K. Miller, V. Y. Glebov, C. Stoeckl, and T. C. Sangster, *Phys. Rev. C* **85**, 061601 (2012).
- ⁸A. B. Zylstra, H. W. Herrmann, M. G. Johnson, Y. H. Kim, J. A. Frenje, G. Hale, C. K. Li, M. Rubery, M. Paris, A. Bacher, C. R. Brune, C. Forrest, V. Y. Glebov, R. Janezic, D. McNabb, A. Nikroo, J. Pino, T. C. Sangster, F. H. Séguin, W. Seka, H. Sio, C. Stoeckl, and R. D. Petrasso, *Phys. Rev. Lett.* **117**, 035002 (2016).
- ⁹P. A. Cherenkov, *Doklady Akademii Nauk SSSR* **2**, 451 (1934).
- ¹⁰J. Mack, R. Berggren, S. Caldwell, S. Evans, J. F. Jr., R. Lerche, J. Oertel, and C. Young, *Nucl. Instr. Meth. Phys. Res. A* **513**, 566 – 572 (2003).
- ¹¹H. W. Herrmann, Y. H. Kim, C. S. Young, V. E. Fatherley, F. E. Lopez, J. A. Oertel, R. M. Malone, M. S. Rubery, C. J. Horsfield, W. Stoeffl, A. B. Zylstra, W. T. Shmayda, and S. H. Batha, *Rev. Sci. Instrum.* **85**, 11E124 (2014).
- ¹²R. Malone, B. Cox, S. Evans, B. Frogget, H. Herrmann, M. Kaufman, Y. Kim, J. Mack, K. McGillivray, M. Palagi, *et al.*, in *Journal of Physics: Conference Series*, Vol. 244 (IOP Publishing, 2010) p. 032052.
- ¹³F. E. Cecil, D. M. Cole, R. Philbin, N. Jarmie, and R. E. Brown, *Phys. Rev. C* **32**, 690–693 (1985).
- ¹⁴M. S. Rubery, C. J. Horsfield, H. Herrmann, Y. Kim, J. M. Mack, C. Young, S. Evans, T. Sedillo, A. McEvoy, S. E. Caldwell, E. Grafil, W. Stoeffl, and J. S. Milnes, *Rev. Sci. Instrum.* **84**, 073504 (2013).
- ¹⁵N. M. Hoffman, H. W. Herrmann, Y. H. Kim, H. H. Hsu, C. J. Horsfield, M. S. Rubery, D. C. Wilson, W. W. Stoeffl, C. S. Young, J. M. Mack, E. K. Miller, E. Grafil, S. C. Evans, T. J. Sedillo, V. Y. Glebov, and T. Duffy, in *EPJ Web of Conferences*, Vol. 59 (EDP Sciences, 2013) p. 13019.
- ¹⁶A. McEvoy, H. Herrmann, Y. Kim, A. Zylstra, C. Young, V. Fatherley, F. Lopez, J. Oertel, T. Sedillo, T. Archuleta, *et al.*, in *Journal of Physics: Conference Series*, Vol. 717 (IOP Publishing, 2016) p. 012109.
- ¹⁷T. Boehly, D. Brown, R. Craxton, *et al.*, “Initial performance results of the OMEGA laser system,” *Optics Communications* **133**, 495–506 (1997).
- ¹⁸V. Y. Glebov, D. D. Meyerhofer, T. C. Sangster, C. Stoeckl, S. Roberts, C. A. Barrera, J. R. Celeste, C. J. Cerjan, L. S. Dauffy, D. C. Eder, R. L. Griffith, S. W. Haan, B. A. Hammel, S. P. Hatchett, N. Izumi, J. R. Kimbrough, J. A. Koch, O. L. Landen, R. A. Lerche, B. J. MacGowan, M. J. Moran, E. W. Ng, T. W. Phillips, P. M. Song, R. Tommasini, B. K. Young, S. E. Caldwell, G. P. Grim, S. C. Evans, J. M. Mack, T. J. Sedillo, M. D. Wilke, D. C. Wilson, C. S. Young, D. Casey, J. A. Frenje, C. K. Li, R. D. Petrasso, F. H. Séguin, J. L. Bourgade, L. Disdier, M. Houry, I. Lantuejoul, O. Landoas, G. A. Chandler, G. W. Cooper, R. J. Leeper, R. E. Olson, C. L. Ruiz, M. A. Sweeney, S. P. Padalino, C. Horsfield, and B. A. Davis, *Rev. Sci. Instrum.* **77**, 10E715 (2006).
- ¹⁹C. J. Forrest, P. B. Radha, V. Y. Glebov, V. N. Goncharov, J. P. Knauer, A. Pruyne, M. Romanofsky, T. C. Sangster, M. J. Shoup, C. Stoeckl, D. T. Casey, M. Gatu-Johnson, and S. Gardner, *Rev. Sci. Instrum.* **83**, 10D919 (2012).
- ²⁰J. Anderson, C. Gardner, J. McClure, M. Nakada, and C. Wong, *Physical Review* **111**, 572 (1958).
- ²¹J. Benveniste, A. Mitchell, C. Schrader, and J. Zenger, *Nuclear Physics* **19**, 448–452 (1960).
- ²²D. Spaargaren and C. Jonker, *Nuclear Physics A* **161**, 354–374 (1971).
- ²³F. H. Séguin, N. Sinenian, M. Rosenberg, A. Zylstra, M. J.-E. Manuel, H. Sio, C. Waugh, H. G. Rinderknecht, M. G. Johnson, J. Frenje, C. K. Li, R. Petrasso, T. C. Sangster, and S. Roberts, *Rev. Sci. Instrum.* **83**, 10D908 (2012).